

## Measurements of the properties of the Higgs-like boson with the CMS experiment at the LHC

P. AZZURRI on behalf of the CMS COLLABORATION

*INFN, Sezione di Pisa - Largo B. Pontecorvo 3, 56127 Pisa, Italy*

ricevuto il 20 Giugno 2013; approvato il 1 Luglio 2013

**Summary.** — Measurements of the properties of the recently discovered Higgs-like boson are presented using data samples recorded by the CMS experiment corresponding to integrated luminosities of up to  $5.1 \text{ fb}^{-1}$  at 7 TeV and up to  $12.2 \text{ fb}^{-1}$  at 8 TeV in proton proton collisions at the LHC. The results combine decay modes in pairs of photons, Z bosons, W bosons, tau leptons and b quarks. The mass of the boson is determined to be  $125.8 \pm 0.4 \text{ (stat.)} \pm 0.4 \text{ (syst.) GeV}$ , and the signal strength at the measured mass is  $\mu = 0.88 \pm 0.21$ , normalized to the standard model expectation. Combined results on couplings, spin and parity reveal a broad agreement with the expectations of a standard model Higgs boson.

PACS 14.80.Bn – Standard-model Higgs bosons.

PACS 13.85.-t – Hadron-induced high- and super-high-energy interactions (energy > 10 GeV).

PACS 29.40.-n – Radiation detectors.

PACS 29.85.Fj – Data analysis.

### 1. – Introduction

In the standard model (SM) the Brout-Englert-Higgs mechanism explains the electroweak symmetry breaking and allows the W and Z gauge bosons to acquire mass. The mechanism predicts the existence of a Higgs scalar boson (H), and its observation was one of the main goals of the LHC physics program.

Results on the properties of the recently observed boson by ATLAS [1] and CMS [2], and its compatibility with the SM Higgs boson are given here, based on proton-proton collisions data samples collected by the CMS experiment [3] corresponding to integrated luminosities of up to  $5.1 \text{ fb}^{-1}$  at 7 TeV and up to  $12.2 \text{ fb}^{-1}$  at 8 TeV. Information has been combined from four production channels and five decay modes [4-6]. The analyzed production channels, in decreasing magnitude, are i) gluon fusion (ggH)  $gg \rightarrow H$ , ii) vector boson fusion (VBF)  $WW, ZZ \rightarrow qqH$ , iii) associated vector production (VH)  $W, Z \rightarrow HW, Z$  and iv) associated top quarks production (ttH)  $gg \rightarrow Ht\bar{t}$ . The searched decay modes are i)  $H \rightarrow ZZ \rightarrow 4\ell$ , ii)  $H \rightarrow \gamma\gamma$ , iii)  $H \rightarrow WW \rightarrow \ell\nu\ell\nu$ , iv)  $H \rightarrow \tau\tau$  and v)  $H \rightarrow b\bar{b}$ .

In the SM all the properties of the Higgs boson are fixed by the values of its mass ( $m_H$ ). The mass of the new boson is measured using the  $4\ell$  and  $\gamma\gamma$  final states, where the experimental mass resolution for  $m_H \simeq 125$  GeV is roughly 1–3%. Using the measured signal strengths in the various production and decay channels, the couplings of the new boson can be extracted. Finally the spin and parity of the new boson are analyzed, making use of the decay distributions in the  $ZZ \rightarrow 4\ell$  channel.

In the following a brief overview of the search channels is given.

- The  $ZZ \rightarrow 4\ell$  analysis [7] searches a signal four-lepton invariant mass peak over a smaller and continuous background, mostly from fully leptonic non-resonant  $ZZ$  diboson decays. Selected events are categorized according to the multiplicity of additional jets, to discriminate ggH production from VBF and VH production.
- The  $\gamma\gamma$  analysis [8, 2] also looks for a signal mass peak, over a smoothly falling background originating from QCD processes with diphotons or misidentified photons. Selected events are classified according to the eventual presence of additional jets or leptons into three categories: ggH (untagged), VBF or VH categories.
- The  $WW \rightarrow \ell\nu\ell\nu$  analysis [9] searches for events with opposite charge isolated leptons and missing transverse energy. Selected events are categorized according to the lepton flavors and to the presence of additional jets (for the VBF categories). An excess of signal events is searched over the main  $WW$  and top-quark background productions.
- The  $\tau\tau$  searches [10] categorizes ditau events based on the decay channel of each tau, and on the presence of additional jets for the VBF categories. Main backgrounds arise from  $Z \rightarrow \tau\tau$ ,  $W$  plus jets and QCD multijet processes, and are estimated with data control samples. Dedicated searches of VH signal productions with tau decays have been performed in events with three or four final state leptons [11].
- The bb decay search in the associated VH channel [12] selects events with weak bosons decaying to leptons ( $Z \rightarrow ee, \mu\mu, \nu\nu$  and  $W \rightarrow e\nu, \mu\nu$ ), and two b-jets from the Higgs boson decay. The main backgrounds arise from  $W/Z$  plus jets processes and top productions, and are estimated from data control samples. The Higgs boson bb decays associated to top-quark pairs have also been searched [13], with semileptonic or fully leptonic top-quark pair decays. In this analysis backgrounds originate from top-pairs with additional QCD jets, and are estimated from theoretical predictions.

## 2. – Signal significance and mass

The presence of Higgs signals is quantified with a test statistics based on the profile likelihood ratio  $q$  [4], depending on a signal strength modifier  $\mu$  to allow for deviations from the SM Higgs predictions. The asymptotic approximation [14] is used to derive the results and nuisance parameters are used to evaluate systematic uncertainties, treated with a frequentist approach.

Signal model parameters, as  $\mu$ , are measured with likelihood ratio profile. The 68% and 95% confidence level (CL) limits on a given parameter are determined with  $q = 1$  and  $q = 3.84$ , respectively. The two dimensional (2D) 68% and 95% contours for pairs of parameters are fixed by the  $q = 2.3$  and  $q = 6$  likelihood ratio values.

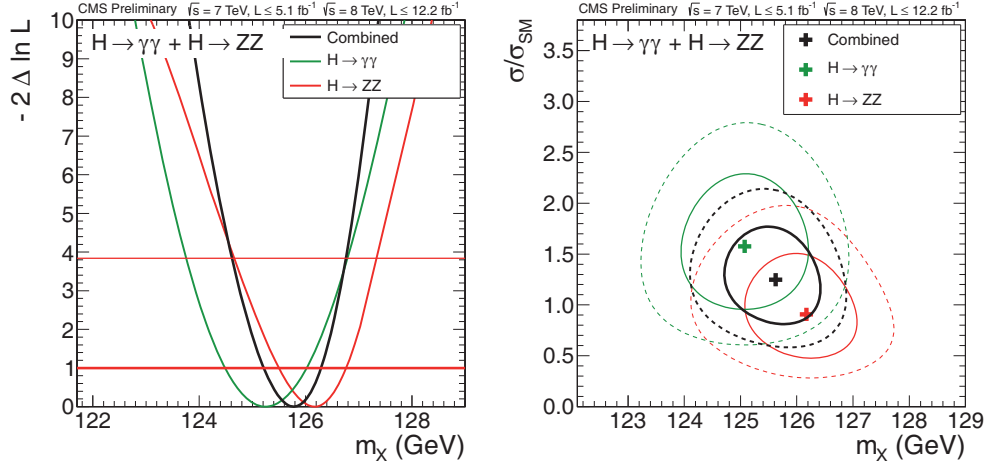


Fig. 1. – (Left) The signal likelihood ratio profile as a function of the boson mass  $q(m_X)$  for the  $\gamma\gamma$  and  $4\ell$  channels separately and combined. (Right) The boson signal strength  $\mu = \sigma/\sigma_{SM}$  versus the boson mass  $m_X$  68% and 95% CL contours.

The local probability ( $p$ -value) is the probability to obtain a  $q$  value at least as large as the one observed in data under the background-only hypothesis. The local significance of the signal, in  $\sigma$  units, is related to the local  $p$ -value through the one-sided Gaussian tail integral convention.

The mass of the observed boson  $m_X$  is measured with the  $\gamma\gamma$  and  $ZZ \rightarrow 4\ell$  channels. Figure 1 shows the observed  $q$  profile as a function of  $m_X$ . The horizontal lines at 1 and 3.8 determine the observed mass 68% and 95% CL intervals, including all systematic uncertainties. The combined mass measurement, with separate statistical and systematic uncertainties is  $m_X = 125.8 \pm 0.4$  (stat.)  $\pm 0.4$  (syst.) GeV.

For a SM Higgs boson with mass 125.8 GeV the observed (median expected) signal significances with the analyzed data samples are: i) 4.4(5.0) $\sigma$  for the  $4\ell$  channel, ii) 3.0(4.3) $\sigma$  for the WW channel, iii) 4.0(2.8) $\sigma$  for the  $\gamma\gamma$  channel, iv) 1.8(2.2) $\sigma$  for the  $\tau\tau$  channel, v) 1.8(2.1) $\sigma$  for the  $bb$  channel, all evaluated with fixed SM signal strength ( $\mu = 1$ ). The overall combined observed significance reaches 6.9 $\sigma$ .

### 3. – Higgs boson signal strength

Using a common signal strength modifier for all combined analysis channels yields an observed value for  $m_H = 125.8$  GeV of  $\mu = \sigma/\sigma_{SM} = 0.88 \pm 0.21$ , compatible with the expected SM value  $\mu = 1$ .

The Higgs boson signal strength for  $m_H = 125.8$  GeV, in different searched channels and decay modes are shown in fig. 2. None of the fitted signal strengths deviates significantly from  $\mu = 1$  and the overall compatibility with the SM expectations with the current sensitivity is good.

To test the strengths of the Higgs boson couplings hypothesis to vector bosons and top quarks, a rough separation between the vector boson fusion and associated vector productions (VBF+VH) versus the gluon fusion and associated top productions (ggH+ttH), has been tested. Figure 3 shows the 68% CL contours of the measured signal strength in the ggH+ttH and VBF+VH production modes, for each of the five decay modes.

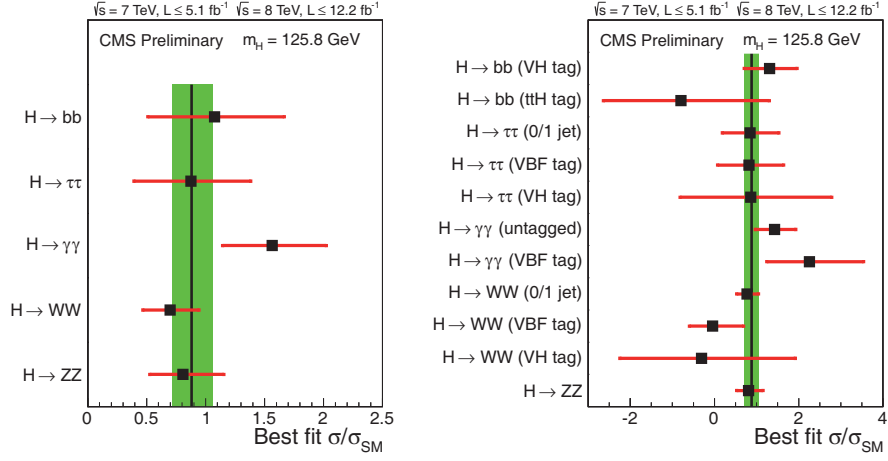


Fig. 2. – Measured Higgs boson signal strengths at  $m_H = 125.8$  GeV, by decay mode (left), and with additional tags targeting particular production mechanisms (right).

#### 4. – Compatibility with standard model Higgs couplings

All production and decay combinations are assumed to be related to the Higgs boson cross-section and decay fraction according to the formula

$$\sigma \times \text{BR}(x \rightarrow H \rightarrow ff) = \sigma_x \cdot \frac{\Gamma_{ff}}{\Gamma_H},$$

where  $x$  is the production mode (ggH, VBF, VH, ttH) and  $ff$  is the final state ( $f = Z, W, \tau, \gamma, b$ ).

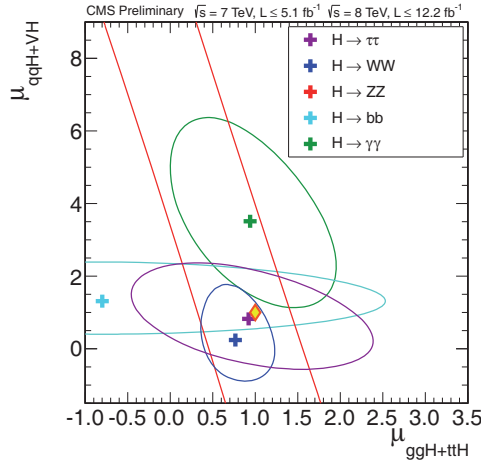


Fig. 3. – Signal strength for ggH+ttH versus VBF+VH production: the curves show 68% CL regions for each decay mode (left).

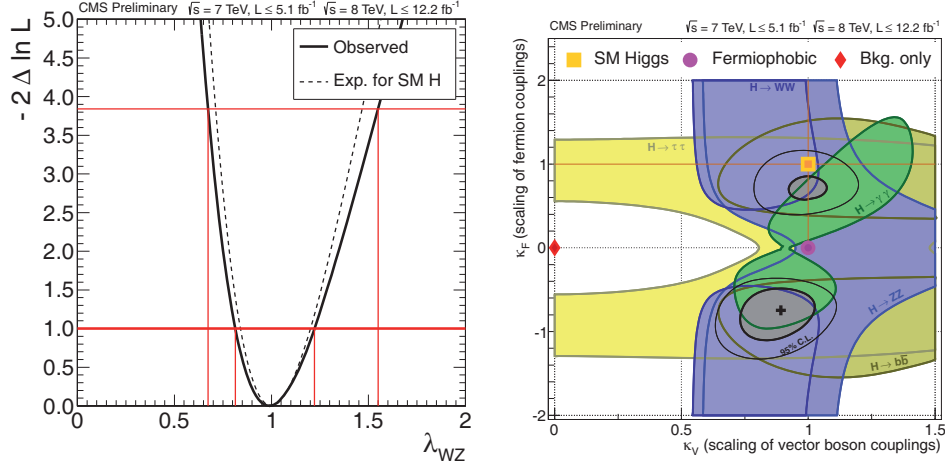


Fig. 4. – Custodial symmetry test: the likelihood ratio  $q$  scan of the coupling modifier ratio  $\lambda_{WZ}$  (left). Vector boson and fermion couplings: 68% CL regions for the  $\kappa_V$  and  $\kappa_f$  coupling modifiers for each decay channel. The cross indicates the global best-fit values.

The gluon fusion production and diphoton decay are generated by loop diagrams, and particularly sensitive to physics beyond the standard model (BSM). Effects of new BSM particles would also modify the total decay width  $\Gamma_H$ . To test the SM Higgs couplings hypothesis in the data, modified couplings strengths  $\kappa_i$  are introduced in the likelihood, and any deviation of  $\kappa_i$  from unity indicates a deviation from the SM Higgs couplings.

**4.1. Custodial symmetry.** – As a test of the relation between the W and Z boson masses and their couplings to the Higgs boson, that are protected against radiative corrections by the “custodial symmetry” property, the value of the ratio  $\lambda_{WZ} = \kappa_W/\kappa_Z$  is accessed. The likelihood scan  $q(\lambda_{WZ})$  is shown in fig. 4, combining all input channels and leaving free the  $\kappa_Z$  and  $\kappa_f$  coupling modifiers: the 95% CL interval for  $\lambda_{WZ}$  obtained from the data is  $[0.67, 1.55]$ .

**4.2. Couplings to vector bosons and fermions.** – An important test of the expected SM couplings is to fit for coupling deviations to vector bosons  $\kappa_V$  (common to W and Z), and to fermions  $\kappa_f$ . Figure 4 shows the interplay of the different decay channels in constraining the  $(\kappa_V, \kappa_f)$  plane, with the 68% CL regions deriving from each decay mode and combined. The obtained 1D 95% CL intervals for  $\kappa_V$  and  $\kappa_f$  are  $[0.78, 1.19]$  and  $[0.40, 1.12]$ , respectively.

**4.3. New physics effects.** – New BSM physics could modify the production and decay rates of the Higgs boson. Loop diagrams, as in gluon fusion productions and diphoton decays, would be particularly sensitive to new effects, and deviations from the SM expectations are quantified with the  $\kappa_g$  and  $\kappa_\gamma$  scale factors. The data results in terms of 68%, 95% and 99.7% CL regions in the  $(\kappa_\gamma, \kappa_g)$  plane are shown in fig. 5. The individual 95% CL regions are  $[0.98, 1.92]$  for  $\kappa_\gamma$  and  $[0.55, 1.07]$  for  $\kappa_g$ . Figure 5 also shows the likelihood profile of an additional BSM decay width, parameterized as  $\text{BR}_{\text{BSM}} = \Gamma_{\text{BSM}}/\Gamma_H$ , with  $\kappa_g$  and  $\kappa_\gamma$  free, yielding the 95% upper limit  $\text{BR}_{\text{BSM}} < 0.62$ .

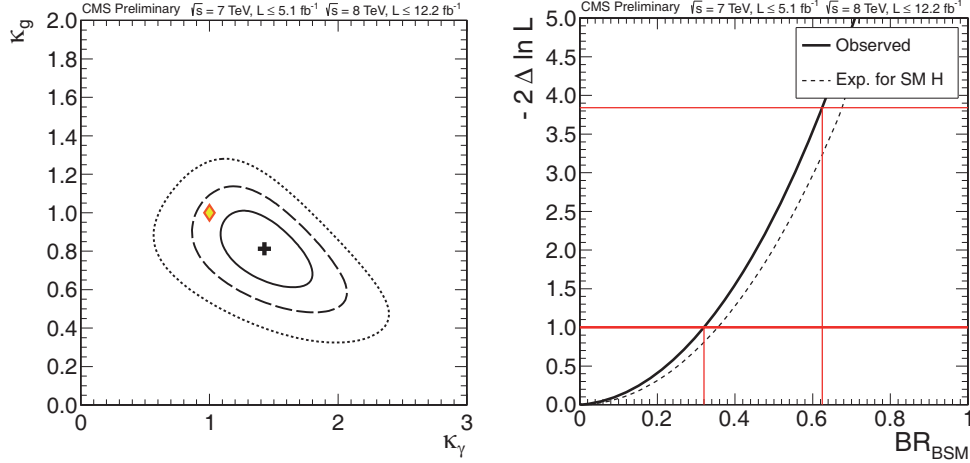


Fig. 5. – The 68%, 95% and 99.7% CL regions in the  $(\kappa_g, \kappa_\gamma)$  plane (right): the cross indicates the best-fit values, and the diamond the SM point. The likelihood ratio  $q$  scan of a new physics branching ratio  $BR_{BSM}$  (left), as observed in the data and expected for  $BR_{BSM} = 0$ .

4.4. *Fermion couplings asymmetries.* – Differences among the fermion couplings, as possible in models with two or more Higgs doublets, are tested in terms of the  $\lambda_{du} = \kappa_d/\kappa_u$  and  $\lambda_{\ell q} = \kappa_\ell/\kappa_q$  coupling modifier ratios, allowing respectively differences in the couplings to down and up fermions, and differences in the couplings to leptons and quarks. The observed 95% CL intervals are  $[0.45, 1.66]$  for  $\lambda_{du}$  and  $[0.00, 2.11]$  for  $\lambda_{\ell q}$ . Figure 6 shows two-dimensional scans of the likelihood ratio in the  $(\lambda_{du}, \kappa_u)$  plane, and in the  $(\lambda_{\ell q}, \kappa_q)$  plane, with the CL regions measured from the data.

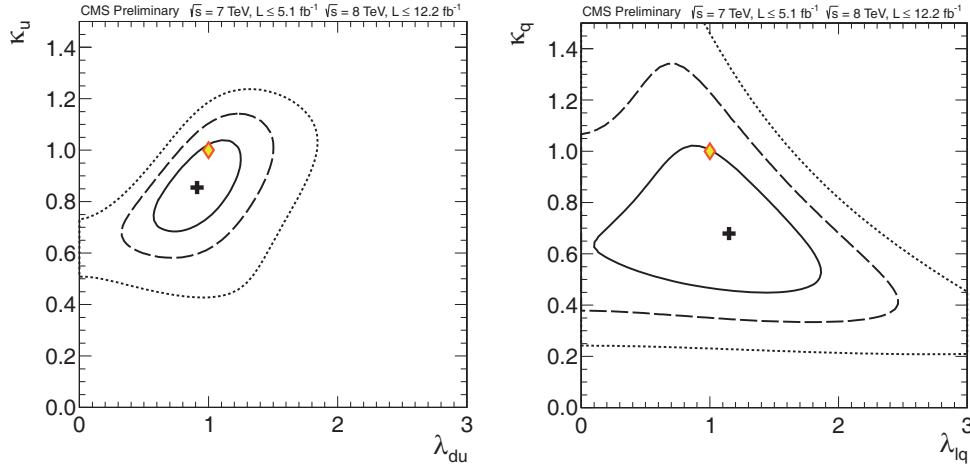


Fig. 6. – The 68%, 95% and 99.7% CL regions in the  $(\lambda_{du}, \kappa_u)$  plane (right): the cross indicates the best-fit values, and the diamond the SM point. The 68%, 95% and 99.7% CL regions in the  $(\lambda_{\ell q}, \kappa_q)$  plane (right): the cross indicates the best-fit values, and the diamond the SM point.

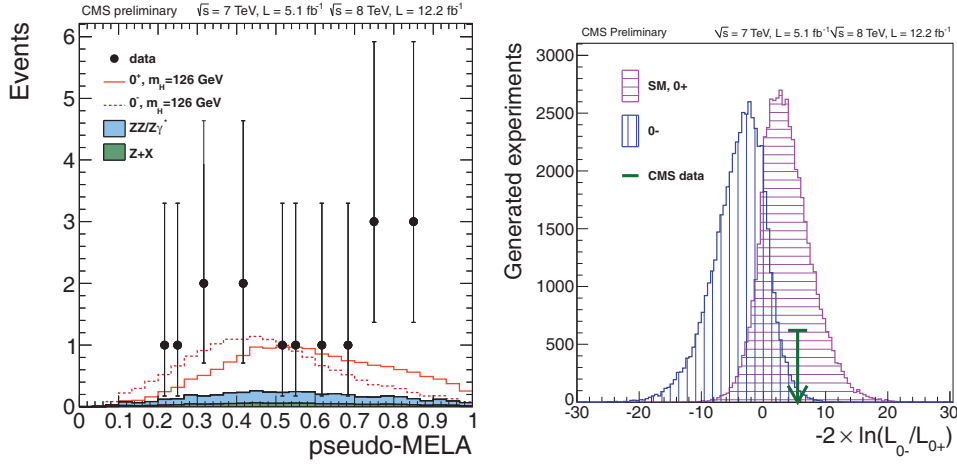


Fig. 7. – Distribution of an optimal kinematic discriminant for  $4\ell$  events to separate the  $J^P = 0^+$  and  $0^-$  signal hypothesis (left): data points with error bars, and expectations for background and the two signal hypothesis, are shown. Signal plus background distributions of a test statistic comparing the SM  $J^P = 0^+$  and  $0^-$  signal hypothesis for  $4\ell$  decays (right): the arrow indicates the value of the test statistic observed in data.

**4.5. Six coupling parameters model.** – Looser tests of a model with six independent couplings  $\kappa_V$ ,  $\kappa_b$ ,  $\kappa_\tau$ ,  $\kappa_t$ ,  $\kappa_g$  and  $\kappa_\gamma$  have been performed, fitting one parameter at a time. The individual couplings modifiers 95% CL intervals obtained from the data are: i)  $[0.58, 1.41]$  for  $\kappa_V$ , ii)  $[0.00, 1.80]$  for  $\kappa_\tau$ , iii)  $[0.43, 1.92]$  for  $\kappa_g$  and iv)  $[0.81, 2.27]$  for  $\kappa_\gamma$ . No 95% CL constrain was obtained for  $\kappa_b$  and  $\kappa_t$ .

## 5. – Analysis of the spin and parity

Investigations of the new discovered boson spin-parity quantum numbers have been performed with  $4\ell$  events [7], making use of the full event kinematical decay information (angles and momenta of reconstructed leptons). The SM  $J^P = 0^+$  hypothesis has been tested against several other  $J^P$  scenarios, and scenarios alternative to the SM are disfavored, with (alternative) signal CL probabilities ( $CL_s$ ) of 2.4% or smaller.

Figure 7, left, shows the distribution of an optimal discriminator for the comparison of the SM  $J^P = 0^+$  hypothesis with a  $J^P = 0^-$  signal hypothesis. The data points show a clear preference for the  $J^P = 0^+$  hypothesis, while the  $J^P = 0^-$  hypothesis is excluded at a level over four standard deviations, and with a  $CL_s$  value smaller than 0.1%. Figure 7, right, shows the post-fit distributions of a test statistic comparing the SM  $J^P = 0^+$  hypothesis with the pseudoscalar signal hypothesis, where the data measurement (indicated by an arrow) disfavors the  $0^-$  hypothesis with a  $CL_s$  value of 2.4%.

## 6. – Conclusions

The properties of the recently discovered boson, and its consistency with the SM Higgs boson have been investigated with the CMS experiment in four production modes and five decay channels, using data samples of up to  $5.1 \text{ fb}^{-1}$  at 7 TeV and up to  $12.2 \text{ fb}^{-1}$

at 8 TeV in proton proton collisions at the LHC. The mass of the new boson is  $125.8 \pm 0.4$  (stat.)  $\pm 0.4$  (syst.) GeV. The combined signal strength is  $0.88 \pm 0.21$  in units of the SM Higgs boson cross section at the measured mass. The measured couplings are consistent with the SM Higgs expectations, within the 20-50% uncertainties. The analysis of the observed decay kinematics strongly disfavors the pure  $J^P = 0^-$  quantum numbers for the signal hypothesis.

## REFERENCES

- [1] ATLAS COLLABORATION, *Phys. Lett. B*, **716** (2012) 1.
- [2] CMS COLLABORATION, *Phys. Lett. B*, **716** (2012) 30.
- [3] CMS COLLABORATION, *JINST*, **03** (2008) S08004.
- [4] CMS COLLABORATION, *Phys. Lett. B*, **26** (2012) .
- [5] CMS COLLABORATION, *Combination of Standard Model Higgs boson searches and measurements of the properties of the new boson with a mass near 125 GeV*, CMS Physics Analysis Summary, CMS-PAS-HIG-12-045 (2012).
- [6] LHC HIGGS CROSS SECTION WORKING GROUP, *LHC HXSWG interim recommendations to explore the coupling structure of a Higgs-like particle*, arXiv:1209.0040 (2012).
- [7] CMS COLLABORATION, *Discovery of a new boson in the search for the standard model Higgs bosons in the  $H \rightarrow ZZ \rightarrow 4\ell$  channel in  $pp$  collisions at  $\sqrt{s} = 7$  and 8 TeV*, CMS Physics Analysis Summary, CMS-PAS-HIG-12-041 (2012).
- [8] CMS COLLABORATION, *Search for a standard model Higgs boson decaying into two photons in  $pp$  collisions*, CMS Physics Analysis Summary, CMS-PAS-HIG-12-015 (2012).
- [9] CMS COLLABORATION, *Evidence for a particle decaying into  $W^+W^-$  in the fully leptonic final state in a standard model Higgs bosons search in  $pp$  collisions at  $\sqrt{s} = 8$  TeV*, CMS Physics Analysis Summary, CMS-PAS-HIG-12-042 (2012).
- [10] CMS COLLABORATION, *Search for standard model Higgs bosons decaying to tau pairs*, CMS Physics Analysis Summary, CMS-PAS-HIG-12-043 (2012).
- [11] CMS COLLABORATION, *Search for a Standard Model Higgs bosons decaying to tau pairs produced in association with a  $W$  or a  $Z$  boson*, CMS Physics Analysis Summary, CMS-PAS-HIG-12-051 (2012).
- [12] CMS COLLABORATION, *Search for standard model Higgs bosons produced in association with  $W$  or  $Z$  bosons, and decaying to bottom quarks*, CMS Physics Analysis Summary, CMS-PAS-HIG-12-044 (2012).
- [13] CMS COLLABORATION, *JHEP*, **05** (2013) 145.
- [14] COWAN G. *et al.*, *Eur. Phys. J. C*, **71** (2011) .